

# Virtual Array for Dual Function MIMO Radar Communication Systems using OTFS Waveforms

Kailong Wang , Athina Petropulu   
Rutgers University, USA

**Abstract**—A MIMO dual-function radar communication (DFRC) system transmitting orthogonal time frequency space (OTFS) waveforms is considered. A key advantage of MIMO radar is its ability to create a virtual array, achieving higher sensing resolution than the physical receive array. In this paper, we propose a novel approach to construct a virtual array for the system under consideration. The transmit antennas can use the Doppler-delay (DD) domain bins in a shared fashion. A number of Time-Frequency (TF) bins, referred to as private bins, are exclusively assigned to specific transmit antennas. The TF signals received on the private bins are orthogonal and thus can be used to synthesize a virtual array, which, combined with coarse knowledge of radar parameters (*i.e.*, angle, range, and velocity), enables high-resolution estimation of those parameters. The introduction of  $N_p$  private bins necessitates a reduction in DD domain symbols, thereby reducing the data rate of each transmit antenna by  $N_p - 1$ . However, even a small number of private bins is sufficient to achieve significant sensing gains with minimal communication rate loss.

## I. INTRODUCTION

An emerging trend in 6G wireless systems [1] is the integration of sensing capabilities on the wireless system hardware platform [2]. Integrated Sensing and Communication (ISAC) [3] devices offer efficient use of hardware and enhanced performance of both sensing and communication functions. Dual-function radar communication systems (DFRC) [4] is a class of ISAC systems that use the same waveform as well as the same hardware for both sensing and communication simultaneously. The dual use makes good utilization of bandwidth and for this reason DFRC systems are particularly attractive in future-generation systems, such as autonomous driving vehicles and unmanned aerial vehicles (UAVs).

Multiple-input multiple-output (MIMO) technology offers significant advantages for communication systems by enabling the formation of flexible beams that can track multiple targets simultaneously. When the transmit waveforms are orthogonal, MIMO radar can synthesize virtual arrays, which have a larger aperture than uniform linear arrays (ULA) with the same number of physical components, thereby improving performance [5]. MIMO systems with orthogonal frequency division multiplexing (OFDM) waveforms can achieve high data rates and reliable communication and have been successfully implemented in the 4G and 5G standards [1]. DFRC MIMO systems using OFDM waveforms have also been explored in [4].

DFRC systems are envisioned to use high frequencies and will be deployed in high-mobility applications (*e.g.* high-speed rail) [1]. In such scenarios, the introduced high Doppler shifts destroy the orthogonality of the OFDM sub-carriers, resulting in Inter-Carrier Interference and performance degradation. Moreover, in high-mobility scenarios, the channel is time-varying and cannot be accurately estimated by its time-frequency representation, making OFDM signal detection challenging. The recently proposed Orthogonal Time Frequency Space (OTFS) waveform [6] overcomes the aforementioned issues. The OTFS system employs Doppler-delay (DD) representation, under which the time-varying channels are sparsely represented and appear linear time invariant [6]. This enables accurate equalization and signal detection in high-mobility scenarios. Existing works have shown that the OTFS outperforms OFDM in high Doppler communication [6], [7], [8].

MIMO wireless systems using OTFS waveform for communication have been studied in [9], where all antennas have unrestricted spectral access and hence the communication rate is maximized. MIMO wireless system using OTFS waveform for sensing is studied in [10]. This work too has all antennas sharing all Delay-doppler(DD) domain bins, which leads to the transmit signals being coupled with the radar target parameters at the radar receiver. In [10], target estimation is performed via coarse Maximum Likelihood Estimation (MLE) detection in the DD domain, followed by iterative target extraction. Although this method efficiently removes the masking effect between targets, the MLE detector has high complexity. MIMO ISAC with OTFS waveforms was recently considered in [11], where the DD bins are assigned to transmit antennas in an exclusive manner. For a single-target scenario, this approach achieves orthogonality at the receiver, enabling the formation of a virtual array for improved target resolution. However, the orthogonality would not hold in a multi-target scenario, and further, exclusive use of DD bins by antennas reduces the communication rate.

In our recent work [12], we proposed a MIMO DFRC system that transmits OTFS waveforms and efficiently uses the available bandwidth for both radar and communication purposes. In [12], the transmit antennas can use the DD bins in a shared fashion, which on one hand, enables high communication rates, on the other hand, makes the sensing task more difficult. In [12], a low-complexity approach was proposed to estimate the radar parameters. However, the target angle resolution in [12] is limited by the size of the

radar receive array.

In this paper, we consider the same system as in [12], and the construction of a virtual array, which along with some coarse target estimates (for example, the estimates obtained in [12]) can significantly improve the system's sensing performance. More specifically, we propose introducing a small number of Time-Frequency (TF) private bins, which are uniquely paired with transmit antennas. The introduction of  $N_p$  private bins necessitates a reduction in DD domain symbols, thereby reducing the data rate of each transmit antenna by  $N_p - 1$ . However, even a small number of private bins is sufficient to achieve significant sensing gains with minimal communication rate loss.

## II. OTFS BACKGROUND

In this section we provide some OTFS background in the context of a single-input single-output communication system.

The system transmits packet bursts, each of duration  $T = N\Delta t$  with bandwidth  $B = M\Delta f$ , where  $N$  is the number of subsymbols,  $M$  is the number of subcarriers,  $\Delta t$  is the subsymbol duration, and  $\Delta f$  is the subcarrier spacing. The orthogonality condition requires that  $\Delta t \cdot \Delta f = 1$  [13]. In each burst, a set of  $NM$  complex symbols are arranged on the DD grid,  $\{(k\Delta\nu, l\Delta\tau) \mid k = 0, 1, \dots, N-1; l = 0, 1, \dots, M-1\}$ , where  $k$  and  $l$  are Doppler and delay indices, respectively. The grid spacing is  $\Delta\nu = 1/(N\Delta t)$  and  $\Delta\tau = 1/(M\Delta f)$ . The transmitted signal is reflected by  $J$  point reflectors, each introducing a Doppler and delay that are integer multiples of the corresponding grid spacing, *i.e.*  $v_j = k_j\Delta\nu$ ,  $k_j \in \mathbb{Z}$  and  $\tau_j = l_j\Delta\tau$ ,  $l_j \in \mathbb{Z}^+$ . The dimensions of the grid are such that can support all present Doppler and delays. The complex gain introduced by each point is  $\beta_j$ .

The OTFS transmitter maps the symbol of DD domain, *i.e.*  $x[k, l]$ , to time-frequency domain, *i.e.*  $X[n, m]$ , via the Inverse Symplectic Finite Fourier Transform (ISFFT) [6],

$$X[n, m] = \frac{1}{NM} \sum_{k=0}^{N-1} \sum_{l=0}^{M-1} x[k, l] e^{j2\pi(\frac{kn}{N} - \frac{ml}{M})}. \quad (1)$$

The analog signal for transmission,  $s(t)$ , is created via the Heisenberg Transform [6], *i.e.*

$$s(t) = \sum_{n=0}^{N-1} \sum_{m=0}^{M-1} X[n, m] g_{tx}(t - n\Delta t) e^{j2\pi m\Delta f(t - n\Delta t)}, \quad (2)$$

where  $g_{tx}(t)$  is the pulse function of the transmitter. The baseband signal,  $s^{k,l}(t)$ , corresponding to  $x[k, l]$  is [3]

$$s^{k,l}(t) = \sum_{n=0}^{N-1} x[k, l] e^{j2\pi \frac{nk}{N}} g_{tx}(t - n\Delta t - \frac{l}{M}\Delta t). \quad (3)$$

Omitting noise, the analog received signal is

$$r(t) = \sum_{j=0}^{J-1} \beta_j s(t - \tau_j) e^{j2\pi v_j(t - \tau_j)}. \quad (4)$$

At the receiver, upon matched filtering and sampling for a duration  $T$  at frequency  $B$  with receiver pulse function  $g_{rx}(t)$  (*a.k.a.* Wigner Transform [6]), the time-frequency domain

samples  $Y[n, m]$  are obtained. Assuming that  $g_{tx}$ ,  $g_{rx}$  are bi-orthogonal, it holds that

$$Y[n, m] = X[n, m] H[n, m], \quad (5)$$

$$H[n, m] = \sum_{j=0}^{J-1} \beta_j e^{-j2\pi v_j \tau_j} e^{j2\pi(v_j n \Delta t - m \Delta f \tau_j)}. \quad (6)$$

The received DD domain symbols,  $y[k, l]$ , can be obtained by applying an SFFT on  $Y[n, m]$ . It holds that as [6]

$$y[k, l] = \sum_{k'=0}^{N-1} \sum_{l'=0}^{M-1} x[k - k', l - l'] h[k', l'], \quad (7)$$

$$h[k, l] = \sum_{j=0}^{J-1} \beta_j e^{-j2\pi \frac{k l_j}{NM}} \delta[k - k_j] \delta[l - l_j]. \quad (8)$$

Substituting eq. (8) into eq. (7) yields [8]

$$y[k, l] = \sum_{j=0}^{J-1} \beta_j e^{-j2\pi \frac{k l_j}{NM}} x[[k - k_j]_N, [l - l_j]_M], \quad (9)$$

where  $[\cdot]_N$  is modular operation with order  $N$ .

Eq (9) can be vectorized as [8]

$$\mathbf{y} = \mathbf{h}\mathbf{x} + \mathbf{w}, \quad (10)$$

where  $\mathbf{y}$ ,  $\mathbf{x}$ , are DD domain vectorized received symbols and transmitted symbols whose  $(l + kM)$ -th element is  $y[k, l]$  and  $x[k, l]$ , respectively;  $\mathbf{w} \in \mathbb{C}^{NM}$  is noise,  $\mathbf{h} \in \mathbb{C}^{NM \times NM}$  is the channel matrix.  $\mathbf{h}$  can be estimated with a single pilot [7], and the information bearing symbols can be estimated via LMMSE equalization.

## III. MIMO DFRC WITH ALL DD BINS USED AS SHARED

Table I: List of Variable Notations

$x_{n_t}[k, l]$	DD transmit symbol on bin $[k, l]$ at antenna $n_t$
$X_{n_t}[n, m]$	TF transmit symbol on bin $[n, m]$ at antenna $n_t$
$s_{n_t}(t)$	Baseband transmit signal at antenna $n_t$
$s_{n_t}^{k,l}(t)$	Baseband transmit signal of symbol on DD bin $[k, l]$
$r_{n_r}(t)$	Baseband receive signal at antenna $n_r$
$r_{n_r}^{k,l}(t)$	Baseband receive signal of symbol on DD bin $[k, l]$
$y_{n_r}[k, l]$	DD receive symbol on bin $[k, l]$ at antenna $n_r$
$Y_{n_r}[n, m]$	TF receive symbol on bin $[n, m]$ at antenna $n_r$
$h[k, l]$	DD domain effective channel of bin $[k, l]$
$H[n, m]$	TF domain effective channel of bin $[n, m]$
$\mathbf{x}_{n_t}/\mathbf{y}_{n_r}$	Vectorized transmit/receive DD domain symbols.
$\mathbf{X}_{n_t}/\mathbf{Y}_{n_r}$	Vectorized transmit/receive TF domain symbols.
$\mathbf{h}/\mathbf{H}$	Vectorized DD/TF channel representation.
$h^j[k, l]/H^j[n, m]$	Effective channel of target $j$
$\omega_j$	Spatial frequency of target $j$
$A_j[k, l]$	DD angle profile of target $j$ on bin $[k, l]$
$\hat{A}_j[k, l]$	Estimated DD angle profile of target $j$ on bin $[k, l]$

Here, we outline the approach of [12] for obtaining limited resolution target estimates. We consider a DFRC system comprising a monostatic MIMO radar with  $N_t$  transmit antennas,  $N_r$  receive antennas and an  $N_c$  antenna communication receiver. The carrier frequency is  $f_c$  Hz, *i.e.*, the wavelength is  $\lambda = c/f_c$  with  $c$  being the speed of light. The transmit and receive antennas form uniform linear arrays (ULA) with spacing  $g_t$  and  $g_r$ , respectively. Due to the multiple transmit and receive antennas, all signals will be indexed by the

operating antenna. The notation used in this section is summarized in table I.

At the transmitter, the modulated binary source data are divided into  $N_t$  parallel streams, one for each transmit antenna. Each antenna constructs and transmits an OTFS waveform.

We assume that all  $NM$  DD and TF bins are available to all transmit antennas to transmit on. Let  $x_{n_t}[k, l]$  be the symbol that the  $n_t$ -th antenna places on the DD bin  $[k, l]$ . Suppose there are  $J_T$  targets in the transmitter far-field, and let  $\theta_j \in [-\frac{\pi}{2}, \frac{\pi}{2}]$ ,  $v_j$ ,  $\tau_j$  be the angle, Doppler and delay corresponding to target  $j$ . We assume that the targets fall on the DD grid. The baseband equivalent of the signal received by the  $n_r$ -th receive antenna corresponding to bin  $[k, l]$  is

$$r_{n_r}^{k,l}(t) = \sum_{j=0}^{J_T-1} \sum_{n_t=0}^{N_t-1} e^{-j2\pi(n_r g_r + n_t g_t) \frac{\sin(\theta_j)}{\lambda}} \sum_{n=0}^{N-1} x_{n_t}[k, l] e^{j2\pi \frac{nk}{N}} \times \beta_j g_{rx}(t - n\Delta t - \frac{l}{M}\Delta t - \tau_j) e^{j2\pi v_j(t - \tau_j)}. \quad (11)$$

In the above, the radar parameters,  $\theta_j, v_j, \tau_j$ , are coupled with the transmitted symbols. While one could use a MLE approach to obtain the radar parameters, this would involve high complexity. Next, we propose a low-complexity estimation approach suitable for practical implementation.

Target angle estimation - The demodulated symbol of the  $n_r$ -th receive antenna corresponding to bin  $[k, l]$  is (see eq (7))

$$y_{n_r}[k, l] = \sum_{j=0}^{J_T-1} \sum_{n_t=0}^{N_t-1} e^{-j2\pi(n_r g_r + n_t g_t) \frac{\sin(\theta_j)}{\lambda}} \sum_{k'=0}^{N-1} \sum_{l'=0}^{M-1} x_{n_t}[k - k', l - l'] h^j[k', l'], \quad (12)$$

$$h^j[k, l] = \beta_j e^{-j2\pi \frac{k l j}{NM}} \delta[k - k_j] \delta[l - l_j]. \quad (13)$$

In the above,  $h^j[k, l]$  is DD domain sensing channel corresponding to the  $j$ -th target. On lumping into  $A_j[k, l]$  all terms of eq. (12) that do not depend on  $n_r$ , we can rewrite eq. (12) as

$$y_{n_r}[k, l] = \sum_{j=0}^{J_T-1} A_j[k, l] e^{-j2\pi n_r \omega_j}, \quad \omega_j = g_r \sin(\theta_j) / \lambda \quad (14)$$

where

$$A_j[k, l] = \sum_{n_t=0}^{N_t-1} e^{-j2\pi n_t g_t \frac{\sin(\theta_j)}{\lambda}} \sum_{k'=0}^{N-1} \sum_{l'=0}^{M-1} x_{n_t}[k - k', l - l'] h^j[k', l']. \quad (15)$$

On assuming that  $N_r > J_T$ ,  $\{y_{n_r}[k, l] \mid n_r = 0, 1, \dots, N_r - 1\}$  can be viewed as the sum of  $J_T$  complex sinusoids with spatial frequencies  $\omega_j(k, l)$  and complex amplitudes  $A_j[k, l]$ . We can estimate the sinusoid frequencies, and thus  $\theta_j$ , via an  $N_r$  point DFT applied on that sequence. The estimation can be repeated across all  $NM$  bins, and this diversity helps achieve high-quality target angle estimates.

Target range and velocity estimation - Since the resolution of the DFT is  $\pi/N_r$ , if  $N_r$  is small there may be multiple

targets corresponding to the estimated angle  $\theta_j$ . If there are  $N_j$  targets, eq. (13) becomes

$$h^j[k, l] = \sum_{q=0}^{N_j-1} \beta_{jq} e^{-j2\pi \frac{k l j q}{NM}} \delta[k - k_{jq}] \delta[l - l_{jq}], \quad (16)$$

where  $\beta_{jq}$ ,  $k_{jq}$ , and  $l_{jq}$  are the coefficient, Doppler index, and delay index of the  $q$ -th target. So  $h^j[k, l]$  contains weighted impulses at points  $(k_{jq}, l_{jq})$ ,  $q = 0, \dots, N_j - 1$ .

Let us define  $A'_j[k, l]$ , based on the known transmitted symbols and the estimated angles, as

$$A'_j[k, l] \triangleq \sum_{n_t=0}^{N_t-1} e^{-j2\pi n_t g_t \frac{\sin(\theta_j)}{\lambda}} x_{n_t}[k, l]. \quad (17)$$

From eq. (15) and eq. (16), it can be seen that  $A_j[k, l]$  is a superposition of multiple versions of  $A'_j[k, l]$  centered at points  $(k_{jq}, l_{jq})$ ,  $q = 0, \dots, N_j - 1$ . Therefore, those points can be found as the location of the peaks of the 2D cross-correlation of  $A_j[k, l]$  and  $A'_j[k, l]$ , leading to target parameters

$$v_{jq} = k_{jq} \Delta v = 2v_{jq} f_c / c, \quad \tau_{jq} = l_{jq} \Delta \tau = 2R_{jq} / c. \quad (18)$$

The ability to resolve targets in the DD domain depends on both the grid spacing and the width of the autocorrelation of  $A'_j[k, l]$ . Based on the DD grid only, the resolution and unambiguous range/velocity are  $R_{res} = \frac{c}{2M\Delta f} [m]$ ,  $R_{max} = \frac{c}{2\Delta f} [m]$ ,  $v_{res} = \frac{c}{2N\Delta t f_c} [m/s]$ ,  $v_{max} = \frac{c}{2\Delta t f_c} [m/s]$ . For a large unambiguous range,  $\Delta f$  needs to be small, which results in a long symbol duration  $\Delta t$ . For a large unambiguous velocity,  $\Delta t$  needs to be small, resulting in a wide  $\Delta f$ .

#### IV. THE PROPOSED VIRTUAL ARRAY FOR IMPROVED SENSING RESOLUTION

In this section, we propose a novel approach to surpass the resolution limits of the radar receive array by creating a virtual array and making selective trade-offs between sensing performance and communication rate. To achieve this, we introduce the concept of *TF domain private bins*, each exclusively paired with a specific transmit antenna.

##### A. Radar sensing

Let us, for simplicity, first present the idea for the case of  $N_t = 2$  transmit antennas. Let bin  $[n_p, m_p]$  be exclusively paired with transmit antenna  $p$  (or otherwise, private to antenna  $p$ ) for  $p = 1, 2$ , and let  $X_p[n, m]$  represent the time-frequency (TF) signal of the  $p$ -th antenna. Since bin  $[n_2, m_2]$  is for use by antenna 2 only, antenna 1 sets  $X_1[n_2, m_2] = 0$ . Similarly, since bin  $[n_1, m_1]$  is for the use of antenna 1 only, antenna 2 sets  $X_2[n_1, m_1] = 0$ .

The TF signal received by radar receive antenna  $n_r$  on private bin  $[n_p, m_p]$  equals (see eq. (5), (6), and fig. 1)

$$Y_{n_r}[n_p, m_p] = \sum_{j=0}^{J_T-1} e^{-j2\pi(n_r g_r + p g_t) \frac{\sin(\theta_j)}{\lambda}} X_p[n_p, m_p] \times \beta_j e^{-j2\pi v_j \tau_j} e^{j2\pi(v_j n_p \Delta t - m_p \Delta f \tau_j)}. \quad p = 1, 2 \quad (19)$$

Placing the ratio  $Y_{n_r}[n_p, m_p] / X_p[n_p, m_p]$  of all receive antennas in vector  $\mathbf{r}_p$ , we get

$$\mathbf{r}_p = \sum_{j=0}^{J_T-1} \beta_j \mathbf{a}_r(\theta_j, v_j, \tau_j; n_p, m_p). \quad (20)$$

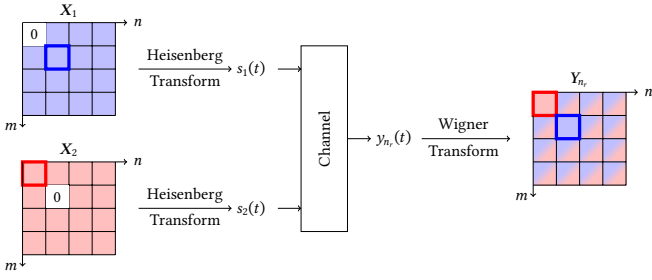


Figure 1: Orthogonal received signals on private TF bins.

$\mathbf{r}_p$  can be viewed as the output of a linear array of size  $N_r$ . By stacking  $\mathbf{r}_1$  and  $\mathbf{r}_2$  into vector  $\mathbf{r}$ , we can formulate an effective virtual array of size  $2N_r$ . Further, we express  $\mathbf{r}$  as

$$\mathbf{r} = [\mathbf{r}_1^T \ \mathbf{r}_2^T]^T = \Phi \boldsymbol{\beta}, \quad (21)$$

where  $\Phi$  is an overcomplete matrix, whose columns are  $[\mathbf{a}_r^T(\tilde{\theta}_j, \tilde{\nu}_j, \tilde{\tau}_j; n_1, m_1) \ \mathbf{a}_r^T(\tilde{\theta}_j, \tilde{\nu}_j, \tilde{\tau}_j; n_2, m_2)]^T$ , with  $(\tilde{\theta}_j, \tilde{\nu}_j, \tilde{\tau}_j)$  corresponding to a grid point of the discretized angle-velocity-delay space. Each element of the vector  $\boldsymbol{\beta}$  corresponds to a grid point in the target space, where a non-zero value indicates the presence of a target at that location, and a zero value indicates no target. Since we already have preliminary target parameters estimated as described in sec. III, we can discretize the target space around those estimates. By restricting the target space to a specific angular region,  $\boldsymbol{\beta}$  becomes a sparse vector, with only a few non-zero elements corresponding to the actual target locations. Therefore, we can solve the following sparse signal recovery (SSR) problem [14] to estimate  $\boldsymbol{\beta}$

$$\min_{\boldsymbol{\beta}} \|\mathbf{r} - \Phi \boldsymbol{\beta}\|_2^2 + \lambda \|\boldsymbol{\beta}\|_1. \quad (22)$$

This design can be generalized to  $N_p$  private bins and  $N_p$  is up to  $N_t$ .

### B. Communication

While modifying (setting to zero) TF domain bins leads to diversity that can be exploited to improve target resolution, it does not allow going back to the DD domain via an ISFFT. Therefore, it has an effect on the set of communication symbols that need to be sent to the communication receiver. To avoid this effect, we propose to restructure the DD domain.

Let each antenna include a zero among its DD-domain symbols. By doing so, each antenna decreases by 1 its information bearing symbols, which are now  $NM - 1$ . Each ISFFT point,  $X_p[n, m]$ , is a linear combination of all the DD domain symbols of the  $p$ th antenna. Even if antenna  $p$  destroys one TF bin by setting it to zero, the remaining  $NM - 1$  bins provide  $NM - 1$  linear combinations of the antenna's  $NM - 1$  DD domain information-bearing symbols.

The ISFFT of  $x_p[k, l]$  can be represented in vector form as

$$\mathbf{X}_p = \mathbf{G} \mathbf{x}_p. \quad (23)$$

$\mathbf{X}_p$  has in its  $(m + nM)$ -th position  $X_p[n, m]$ ;  $\mathbf{x}_p$  has in its  $(l + kM)$ -th position  $x_p(k, l)$ ;  $\mathbf{G} = (\mathbf{F}_N^H \otimes \mathbf{F}_M)$ , with  $\mathbf{F}_M$  being an  $M$ -point DFT matrix; and  $\otimes$  denoting Kronecker product.

Continuing with the  $N_r = 2$  antenna case, we define vector  $\tilde{\mathbf{X}}_1$  to be constructed from  $\mathbf{X}_1$  by excluding  $X_1[n_2, m_2]$  (i.e., containing the RF symbols shown in blue color in fig. 1). As long as antenna 1 had set  $x_1[k_0, l_0] = 0$ , for some  $k_0, l_0$ , its non-zero DD bins can be obtained from  $\tilde{\mathbf{X}}_1$  as

$$\tilde{\mathbf{x}}_1 = \mathbf{C}_1^{-1} \tilde{\mathbf{X}}_1. \quad (24)$$

In the above,  $\tilde{\mathbf{x}}_1$  is constructed from  $\mathbf{x}_1$  by excluding  $x_1[k_0, l_0]$ , and  $\mathbf{C}_1$  is constructed based on  $\mathbf{G}$ , by removing its  $(m_2 + n_2M)$ -th row and its  $(l_0 + k_0M)$ -th column.

In the more general case, where private TF bins are assigned to  $N_p$  (out of the  $N_t$ ) transmit antennas,  $N_p - 1$  zeros need to be inserted in each transmit antenna's TF signal. To ensure recovery of the antenna's information-bearing symbols,  $N_p - 1$  DD domain symbols need to be set to zero for each transmit antenna as well. Thus, in order to refine the sensing resolution by  $N_p$ , the total number of information bearing symbols are reduced to  $N_t NM - N_p(N_t - 1)$ . As will be shown in the simulations section, significant sensing benefit can be achieved with a small  $N_p$ .

Assuming that  $N_c \geq N_t$ , and after performing demodulation, the DD domain I/O across all receive antennas can be expressed as in eq.(10).

$$\begin{bmatrix} \mathbf{y}_1 \\ \vdots \\ \mathbf{y}_{N_c} \end{bmatrix} = \underbrace{\begin{bmatrix} \mathbf{h}_{(1,1)} & \cdots & \mathbf{h}_{(1,N_t)} \\ \vdots & \ddots & \vdots \\ \mathbf{h}_{(N_c,1)} & \cdots & \mathbf{h}_{(N_c,N_t)} \end{bmatrix}}_{\mathbf{h}_{MIMO} \in \mathbb{C}^{N_c N_t \times N_t N_t}} \underbrace{\begin{bmatrix} \mathbf{x}_1 \\ \vdots \\ \mathbf{x}_{N_t} \end{bmatrix}}_{\mathbf{x}_{MIMO} \in \mathbb{C}^{N_t N_t}} + \underbrace{\begin{bmatrix} \mathbf{w}_1 \\ \vdots \\ \mathbf{w}_{N_c} \end{bmatrix}}_{\mathbf{w}_{MIMO} \in \mathbb{C}^{N_c N_t}},$$

where  $\mathbf{h}_{MIMO}$  is the MIMO DD effective channel matrix with  $N_c \times N_t$  blocks and each block is the DD effective channel matrix  $\mathbf{h}_{(n_c, n_t)}$  between the  $n_c$  receive antenna and the  $n_t$  transmit antenna as defined in eq. (10). On assuming every  $\mathbf{h}_{(n_c, n_t)}$  has been estimated via a pilot, the symbol vector  $\hat{\mathbf{x}}_{n_t}$  for all  $n_t$ , can be estimated via LMMSE equalization.

Based on  $\hat{\mathbf{x}}_{n_t}$ , the information bearing symbols can be obtained by taking an ISFFT to get to the TF domain, extracting the nonzero TF bins, and then applying eq.(24). This assumes knowledge of where the zero bins in the DD and TF domains are.

Compared to the MIMO communication system without shared bins, the proposed system increases the number of bits transmitted in one period by at most a factor of  $N_t$ . The communication rate grows linearly with the grid size,  $N$  and  $M$ , which also enhances sensing resolution. However, larger grid sizes increase equalization complexity, so careful selection of system parameters is essential in DFRC MIMO OTFS system design.

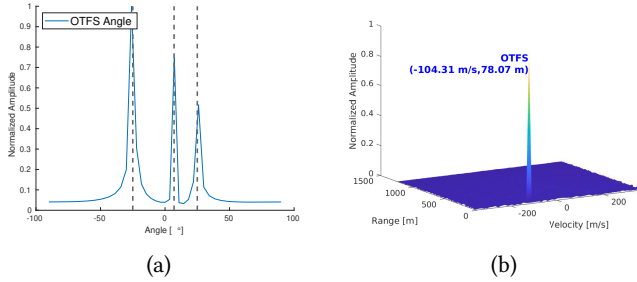


Figure 2: Radar performance of the OTFS system with all DD bins used as shared. Fig. 2a shows angle estimation with ground truth indicated by black dash lines. Fig. 2b shows the 2D Cross-correlation corresponding to the second target.

## V. SIMULATION RESULTS

Table II: System Parameters

Symbol	Parameter	Value
$M$	Number of subcarriers	128
$N$	Number of subsymbols	64
$\Delta f$	Subcarrier spacing	120 KHz
$f_c$	Carrier frequency	24.25 GHz
$g_t$	Transmit antenna spacing	$0.5\lambda$
$g_r$	Receive antenna spacing	$0.5\lambda$

In this section, we present simulation results to demonstrate the performance of the proposed virtual array. The simulated system parameters follow the 5G NR high-frequency standard [15] and are shown in table II. The high-Doppler channel is simulated by the Matlab function [16] with target-*s*/paths parameters shown in table III, IV. The sensing channel contains 3 targets. The communication channel contains 3 paths, and different pairs of transmit and communication antennas have different complex path gains. The information symbols are QPSK, the signal-to-noise ratio (SNR) is 20 dB, and the guard interval is a cyclic prefix with the length equal to the maximum delay introduced by the targets.

Table III: Channel Parameters

Symbol	Parameter	Value
$J$	Number of targets/paths	3
$\theta_j$	Angle of targets/paths	$[-25, 7, 15]^\circ$
$R_j$	Range of targets/paths	$[68.31, 78.07, 48.79]$ m
$v_j$	Velocity of targets/paths	$[57.95, -104.31, 81.13]$ m/s

### A. Sensing with all DD bins used as shared

The targets/paths parameters are as shown in table III,  $N_t = 4$ ,  $N_r = 32$ . In this case, all targets are well separated. The target angles were estimated via the DFT approach described in sec. III, and the result is shown in fig. 2a. The range and velocity of the 2nd target was estimated via the 2D cross-correlation approach of sec. III and is shown in fig. 2b.

Table IV: Channel Parameters

Symbol	Parameter	Value
$J$	Number of targets/paths	3
$\theta_j$	Angle of targets/paths	$[17, 13, 15]^\circ$
$R_j$	Range of targets/paths	$[68.31, 48.79, 78.07]$ m
$v_j$	Velocity of targets/paths	$[46.36, -139.08, 81.13]$ m/s

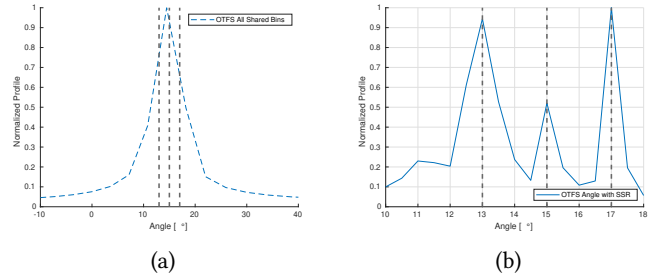


Figure 3: Resolution of DFT- and SSR-based angle estimation.

### B. Trading off Communication for Sensing Using Private Bins

We take  $N_t = 4$ ,  $N_r = 32$ . When the targets are closely spaced in angle, their resolvability depends on the resolution of the receive array, which for  $N_r = 32$  is  $\pi/N_r = 5.625^\circ$ . Here, the channel parameters are shown in table IV. With three targets located within  $2^\circ$ , only one peak is visible in the DFT, as shown in fig. 3a. Next, we use the private bins designed as described in sec. IV, to formulate and solve an SSR problem to refine angle estimation.

We used 4 private bins. Specifically, for each transmit antenna, we set the DD bins  $[0, 0]$ ,  $[1, 1]$ , and  $[2, 2]$ , to zero and placed symbols on the remaining DD grid. After performing the ISFFT, we obtained the TF domain signal and introduced TF private bins at positions  $[0, 0]$ ,  $[1, 1]$ ,  $[2, 2]$  and  $[3, 3]$ . Each transmit antenna was assigned one TF private bin, while the remaining 3 bins were set to zero. We then formulated the SSR problem with the help of the signal received on the private TF bins. Upon solving the SSR problem, the peaks align accurately with the ground truth, as demonstrated in fig. 3b. In our simulations, we set  $\lambda = 10^{-5}$ , which balances resolution and computation effectively.

The discretization of the target space is a critical factor in resolving multiple targets. If the discretization is too coarse, multiple targets may still fall into the same bin. To address this, we propose an iterative refinement mechanism. In our simulations, we initially set the angular spacing to  $d_\alpha = \lfloor \pi/2N_r \rfloor^\circ$ . We then run the SSR detector and iteratively remove the peak with the highest magnitude. If a peak reappears at the same angular bin but corresponds to different Doppler and delay bins during the iteration, it indicates that the grid spacing is too coarse. In such cases, we refine the spacing to  $d_{\alpha+1} = d_\alpha/2$  and rerun the detector. The process continues until all targets are resolved.

Next, we illustrate how the number of private bins and angle space discretization can affect the detection probability of the SSR approach. We performed 100 Monte Carlo simulations; in each simulation 3 targets, separated

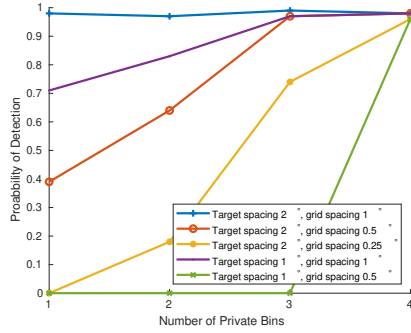


Figure 4: SSR Angle Detection Capability.

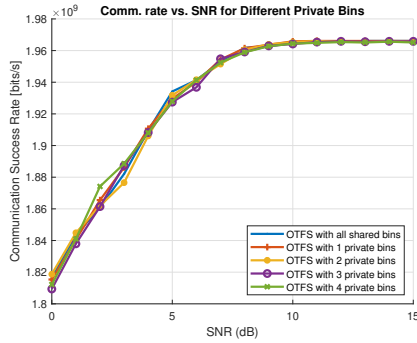


Figure 5: Communication Rate Loss Using Private Bins.

in angle by at least  $2^\circ$  were randomly placed in the angle space  $[-60, 60]^\circ$ . The experiment was repeated for different number of private bins and different levels of angle space discretization. The probability of detection versus number of private bins is shown in fig. 4. The experiment was repeated for 3 target separated in angle by at least  $1^\circ$  and the result is also shown in fig. 4. We can observe that increasing the number of private bins greatly improves the probability of detection, as it increases the number of rows in  $\Phi$ . Also, finer discretization does not always lead to better detection, as it may increase the coherence of  $\Phi$ . Finally, we observe that when the targets minimal angle separation is  $2^\circ$ , it is possible to achieve perfect detection with only 1 private bin.

### C. Communication of the proposed system

We evaluated the communication rate of the proposed system with different numbers of private bins under different SNRs. For the case of  $N_t = 4$ ,  $N_c = 8$ , as shown in fig. 5, the private bin design has similar communication performance compared to the all shared bin design. The loss of communication rate due to the use of private bins is rather small. With  $N_t = 4$  and using QPSK symbols, each private bin leads to  $3 \times \log_2(4) \times 120\text{kHz} = 7.2 \times 10^5$  [bits/s] communication loss. When 4 private bins are used, the percentage communication rate loss is  $\frac{N_t \times (4-1)}{N_t \times NM} = 0.037\%$ .

## VI. CONCLUSION

We have proposed a novel DFRC MIMO OTFS system that is robust to Doppler shifts, can efficiently use the bandwidth for communication and sensing, and is equipped with a low-complexity high-resolution radar parameter estimator. DD domain bins are used in a shared fashion, while some TF bins are private to a small number of transmit antennas. The shared bins enable high communication rates. Introducing private bins requires some reduction of the DD domain symbols transmitted by each antenna. However, it enables the formation of a virtual array that improves the sensing performance. A small number of private bins, or equivalently, a very small amount of rate loss, suffices to achieve significant sensing gains.

## REFERENCES

- [1] W. Saad, M. Bennis, and M. Chen, "A vision of 6g wireless systems: Applications, trends, technologies, and open research problems," *IEEE Network*, vol. 34, no. 3, pp. 134–142, 2020.
- [2] "BLOG | Samsung Research," Aug. 2024, [Online; accessed 10. Aug. 2024].
- [3] M. Ubadah, S. K. Mohammed, R. Hadani, S. Kons, A. Chockalingam, and R. Calderbank, "Zak-ofds for integration of sensing and communication," *arXiv.org*, 2024.
- [4] Z. Xu and A. Petropulu, "A bandwidth efficient dual-function radar communication system based on a mimo radar using ofdm waveforms," *IEEE Transactions on Signal Processing*, vol. 71, pp. 401–416, 2023.
- [5] Y. Liu, G. Liao, and Z. Yang, "Range and angle estimation for mimo-ofdm integrated radar and communication systems," in *2016 CIE International Conference on Radar (RADAR)*, 2016, pp. 1–4.
- [6] R. Hadani, S. Rakib, M. Tsatsanis, A. Monk, A. J. Goldsmith, A. F. Molisch, and R. Calderbank, "Orthogonal time frequency space modulation," in *2017 IEEE Wireless Communications and Networking Conference (WCNC)*, 2017, pp. 1–6.
- [7] Y. Hong, T. Thaj, and E. Viterbo, *Delay-Doppler Communications*, Elsevier Science, 2022.
- [8] P. Raviteja, K. T. Phan, Y. Hong, and E. Viterbo, "Interference cancellation and iterative detection for orthogonal time frequency space modulation," *IEEE Transactions on Wireless Communications*, vol. 17, no. 10, pp. 6501–6515, 2018.
- [9] M. Kollengode Ramachandran and A. Chockalingam, "Mimo-ofds in high-doppler fading channels: Signal detection and channel estimation," in *2018 IEEE Global Communications Conference (GLOBECOM)*, 2018, pp. 206–212.
- [10] L. Gaudio, M. Kobayashi, G. Caire, and G. Colavolpe, "Hybrid digital-analog beamforming and mimo radar with ofds modulation," *ArXiv*, vol. abs/2009.08785, 2020.
- [11] M.F. Keskin, C. Marcus, O. Eriksson, A. Alvarado, J. Widmer, and H. Wymeersch, "Integrated sensing and communications with mimo-ofds," *arXiv.org*, 2023.
- [12] K. Wang and A. Petropulu, "A bandwidth efficient dual function radar communication system based on a mimo radar using ofds waveforms," Submitted to 2025 IEEE International Conference on Acoustics, Speech and Signal Processing (ICASSP).
- [13] S.K. Mohammed, "Derivation of ofds modulation from first principles," *IEEE Transactions on Vehicular Technology*, vol. 70, no. 8, pp. 7619–7636, 2021.
- [14] S. Kalogerias and A. Petropulu, "Matrix completion in colocated mimo radar: Recoverability, bounds & theoretical guarantees," *IEEE Transactions on Signal Processing*, vol. 62, no. 2, pp. 309–321, 2014.
- [15] W. Vook, A. Ghosh, E. Diarte, and M. Murphy, "5g new radio: Overview and performance," in *2018 52nd Asilomar Conference on Signals, Systems, and Computers*, 2018, pp. 1247–1251.
- [16] "OTFSModulationExample," June 2024, [Online; accessed 24. Jun. 2024].